

Podocin is translocated to cytoplasm in
Puromycin Aminonucleoside Nephrosis rats and
in poor prognosis patients with IgA nephropathy

メタデータ	言語: English 出版者: 公開日: 2015-03-20 キーワード (Ja): キーワード (En): 作成者: 福田, 裕光 メールアドレス: 所属:
URL	https://jair.repo.nii.ac.jp/records/2001791



Podocin is translocated to cytoplasm in Puromycin Aminonucleoside Nephrosis rats and in poor prognosis patients with IgA nephropathy

Journal:	<i>Cell and Tissue Research</i>
Manuscript ID:	CTR-14-0397.R2
Manuscript Type:	Regular Article
Date Submitted by the Author:	n/a
Complete List of Authors:	Fukuda, Hiromitsu; Juntendo University School of Medicine, Division of Nephrology, Internal Medicine Hidaka, Teruo; Juntendo University School of Medicine, Division of Nephrology, Internal Medicine Takagi-Akiba, Miyuki; Juntendo University School of Medicine, Division of Nephrology, Internal Medicine Ichimura, Koichiro; Juntendo University School of Medicine, Anatomy Trejo, Juan; Juntendo University School of Medicine, Division of Nephrology, Internal Medicine Sasaki, Yu; Juntendo University School of Medicine, Division of Nephrology, Internal Medicine Wang, Juan; Juntendo University School of Medicine, Division of Nephrology, Internal Medicine Sakai, Tatsuo; Juntendo University School of Medicine, Anatomy Asanuma, Katsuhiko; Kyoto university Graduate School of Medicine, Medical Innovation Center, Laboratory for kidney research (TMK project) Tomino, Yasuhiko; Juntendo University School of Medicine, Division of Nephrology, Internal Medicine
Keywords:	podocyte, podocin, synaptopodin, IgA nephropathy, Puromycin Aminonucleoside Nephrosis rats

1
2
3
4
5 CELL & TISSUE RESEARCH Editor
6 Prof. Klaus Unsicker: Coordinating Editor
7 Dr. Joseph V. Bonventre: Section Editor
8

9 Dear Prof. Unsicker and Dr. Bonventre
10

11 Thank you for your management of our previous submission. We really appreciate
12 your consideration of our manuscript. We were able to recompose more
13 sophisticated figures with Mr. Andreas Schober (CTR-Editorial Office) suggestions.
14 Following his suggestions, we revised our manuscript and adjusted the legends to
15 the new figures. We hope that the figures and the edited manuscript have
16 improved in such a manner that it can now be considered acceptable for publication.
17
18

19 On behalf of all the authors, I would like to ask you to consider our revised
20 manuscript entitled "Podocin is translocated to cytoplasm in Puromycin
21 Aminonucleoside Nephrosis rats and in poor prognosis patients with IgA
22 nephropathy" for publication in Cell and Tissue Research as an original research
23 article. In this pathology study we investigated about glomerulonephritis, focusing
24 on podocyte injury. All study participants provided informed consent, and the study
25 design was approved by our institute's ethics review board. Glomerulonephritis
26 produces various symptoms and also has different reactions to treatments. We
27 focused on the staining gap of podocytes proteins: podocin and synaptopodin.
28

29 Our results showed that the podocin and synaptopodin staining pattern was
30 different, especially in irreversible glomerulonephritis, and we also found that
31 podocin was translocated to the cytosol of podocytes by endocytosis. We feel that
32 the findings from this study will be of special interest to the readers of Cell and
33 Tissue Research.
34

35 This manuscript has not been published and is not under consideration for
36 publication elsewhere. All the authors have read the manuscript and have
37 approved this submission.
38
39

40 Sincerely,
41

42 Teruo Hidaka, M.D. Ph.D
43 Yasuhiko Tomino, M.D.
44 Division of Nephrology, Department of Internal Medicine,
45 Juntendo University school of medicine.
46 2-1-1 Hongo, Bunkyo-City, Tokyo, JAPAN
47 TEL: +81-3-3813-3111
48 FAX: +81-3-3813-1183
49
50
51
52
53
54
55
56
57
58
59
60

1 [Title]

2 Podocin is translocated to cytoplasm in Puromycin Aminonucleoside Nephrosis rats
3 and in poor prognosis patients with IgA nephropathy

4 [Author]

5 Hiromitsu Fukuda^{1, 5}, Teruo Hidaka^{1, 5}, Miyuki Takagi-Akiba¹, Koichiro Ichimura³,
6 Juan Alejandro Oliva Trejo¹, Yu Sasaki¹, Juan Wang^{1, 4}, Tatsuo Sakai³, Katsuhiko
7 Asanuma^{1,2}, Yasuhiko Tomino¹

8 [Institution]

9 1. Division of Nephrology, Department of Internal Medicine, Juntendo University
10 Faculty of Medicine, Tokyo, Japan

11 2. Medical Innovation Center, Laboratory for Kidney Research (TMK project),
12 Kyoto University Graduate School of Medicine, Kyoto, Japan

13 3. Department of Anatomy, Juntendo University School of Medicine, Tokyo, Japan

14 4. Department of Nephrology, The First Hospital, China Medical University,
15 Shenyang, China

16 5. H.F. and T.H. contributed equally to this article.

17
18 Address correspondence to:

19 Yasuhiko Tomino, M.D. Division of Nephrology, Department of
20 Internal Medicine, Juntendo University Faculty of Medicine 2-1-1, Hongo,
21 Bunkyo-ku, Tokyo 113-8421, Japan

22 Tel: +81-3-3813-3111 Fax: +81-3-3813-1183

23 e-mail: yasu@juntendo.ac.jp

24

25

26

27

28

29

30

1
2
3
4
5 266
7 278
9 [Abstract]

10 28 [Abstract]
11 29 Podocytes serve as the final barrier to urinary protein loss through a
12 30 highly specialized structure called a slit membrane, and maintain foot process and
13 31 glomerular basement membranes. Podocyte injury results in progressive
14 32 glomerular damage and accelerates sclerotic changes, although the exact
15 33 mechanism of podocyte injury is still obscure. We focused on the staining gap
16 34 (podocin gap) defined as the staining difference between podocin and synaptopodin,
17 35 which are normally located in the foot process. In puromycin aminonucleoside
18 36 nephrosis rats, the podocin gap is significantly increased ($p < 0.05$) and podocin is
19 37 translocated to the cytoplasm on days 7 and 14 but not on day 28. Surprisingly, the
20 38 gap is also significantly increased ($p < 0.05$) in human kidney biopsy specimens of
21 39 poor prognosis IgA nephropathy patients. This suggests that the podocin gap could
22 40 be a useful marker for classifying the prognosis of IgA nephropathy and indicating
23 41 the translocation of podocin to the cytoplasm. Next, we found more evidence of
24 42 podocin trafficking in podocytes where podocin merged with Rab5 in puromycin
25 43 aminonucleoside nephrosis rats at day 14. In immunoelectron microscopy, the
26 44 podocin positive area was significantly translocated from the foot process areas to
27 45 the cytoplasm ($p < 0.05$) on days 7 and 14 in puromycin aminonucleoside nephrosis
28 46 rats. Interestingly, podocin is also translocated to the cytoplasm in poor-prognosis
29 47 human IgA nephropathy.

30 48 In this paper, we demonstrated that the translocation of podocin by
31 49 endocytosis could be a key traffic event of critical podocyte injury and that the
32 50 podocin gap could indicate the prognosis of IgA nephropathy.
33
34
35
36
37
38
39
40
41
42
43
44
45
46
47
48
49
50
51
52
53
54
55
56
57
58
59
60

For Peer Review

1
2
3
4
5
6
7
8
9
10
11
12
13
14
15
16
17
18
19
20
21
22
23
24
25
26
27
28
29
30
31
32
33
34
35
36
37
38
39
40
41
42
43
44
45
46
47
48
49
50
51
52
53
54
55
56
57
58
59
60

1
2
3
4
5 52 [Introduction]

6
7 53 Podocytes are specialized epithelial cells constituting an essential part of
8
9
10 54 the glomerular filtration barrier. Their interdigitated foot processes, connected by a
11
12 55 slit diaphragm (SD), together with fenestrated endothelial cells and an intervening
13
14 56 basement membrane, form the filtration barrier. The importance of podocyte
15
16 57 integrity in the pathogenesis of nephrotic syndrome is best illustrated by the
17
18 58 identification of human diseases causing mutations in genes encoding nephrin,
19
20 59 podocin, and CD2AP that span and stitch together foot processes of neighboring
21
22 60 podocytes (1–3).
23

24
25 61 In the podocyte, podocin localizes in the SD, where it is assumed to act as
26
27 62 an intercellular scaffold protein, assembling SD components in lipid raft associated
28
29 63 microdomains (4,5). Podocin is a membrane-attached protein and it is predicted to
30
31 64 form a hairpin-like structure, with both N- and C- terminuses residing in the
32
33 65 cytoplasm (6). NPHS2 mutations cause several diseases with an interference of
34
35 66 podocin intercellular trafficking (7).
36

37
38 67 In mammalian cells, endocytosis is mediated via two principal routes, i.e.
39
40 68 clathrin-mediated endocytosis (CME) and clathrin-independent, raft-mediated
41
42 69 endocytosis (RME) (8). CME targets proteins to the early endosome, a sorting
43
44 70 station directing vesicles to either recycling or degradation. Besides this classic
45
46 71 CME pathway, RME has recently been the focus of intensive research, uncovering
47
48 72 the new concept that the microdomain itself behaves as a vehicle for
49
50 73 internalization. RME is generally defined by its clathrin independence, cholesterol
51
52 74 sensitivity, and a typical morphology of smooth invaginations (9).
53

54
55 75 Shono et al. demonstrated that podocin co-localizes with the coxsackie virus
56
57 76 and adeno virus receptor (CAR) and with ZO-1 at the tight junction between foot
58
59
60

1
2
3
4
5 77 processes in puromycin aminonucleoside (PA) nephrosis (PAN) rat kidneys and
6
7 78 podocin facilitated the coalescence of lipid rafts containing CAR, and makes
8
9 79 dynamic cytoskeletal arrangement (10). They also demonstrated that podocin and
10
11 80 CAR exhibit a diffuse punctate pattern throughout the cytoplasm in both proteins'
12
13 81 co-transfected COS-7 cells.
14

15
16 82 Regarding PAN, the intraperitoneal injection of PA to rats is an
17
18 83 experimental model characterized by massive proteinuria and by marked
19
20 84 morphological changes in podocytes, including the effacement of foot processes
21
22 85 their focal adhesion with Bowman's capsules and the focal detachment from the
23
24 86 GBM (11–13). Thus, PA-induced nephrosis is regarded as an experimental model of
25
26 87 human nephrotic syndrome and glomerulosclerosis.
27

28
29 88 In this paper, we have demonstrated that podocin is translocated to the
30
31 89 cytoplasm by endocytosis in both the PAN rat model and in poor-prognosis human
32
33 90 immunoglobulin A nephropathy (IgAN) specimens using the difference in the
34
35 91 staining of podocin and synaptopodin (synpo). This novel approach shows that
36
37 92 podocin is translocated to the cytoplasm in the human nephropathy specimens and
38
39 93 may help advance the-understanding of podocin endocytosis.
40

41 94
42
43
44
45
46
47
48
49
50
51
52
53
54
55
56
57
58
59
60

1
2
3
4
5 95 [Materials & Methods]
6

7 96 ***Antibodies***
8

9 97 The monoclonal mouse anti-synaptopodin antibody (Progen, Heidelberg,
10 98 Germany), Alexa 488 conjugated donkey anti-rabbit IgG antiserum (Invitrogen,
11 99 California, USA), Alexa 555 conjugated goat anti-mouse IgG antiserum (Invitrogen,
12 100 California, USA), mouse monoclonal Rab5 antibody (#50523 Abcam, Japan) and
13 101 the 5 nm colloidal- gold-conjugated goat anti-rabbit IgG antiserum (heavy and
14 102 light) (BB international, Cardiff, UK) were purchased for immunohistochemistry
15 103 and/or immunoelectron microscopy. Polyclonal rabbit anti-podocin antiserum has
16 104 been described previously (6).
17
18
19
20
21
22
23
24
25
26
27

28 106 ***Experimental animals***
29

30 107 Adult male Sprague-Dawley rats (weighing about 200 g) were obtained
31 108 from Sankyo laboratory service (Tokyo, Japan).
32
33
34

35 109 For PAN, a single dose (15 mg / 100 g BW) of PA (Sigma, St. Louis, USA)
36 110 was injected intraperitoneally into the rats to induce a nephrotic state, as
37 111 described previously (14,15). These rats were housed under specific pathogen free
38 112 (SPF) conditions using individual metabolic cages with free access to standard
39 113 chow and drinking water. 24-hour urine was collected once a week throughout the
40 114 experiments. Urinary albumin, urinary total protein, and creatinine were
41 115 measured by the same methods as clinical examination. All experiments were
42 116 performed according to the guidelines of the Committee on Animal Experiments of
43 117 Juntendo University, Tokyo, Japan.
44
45
46
47
48
49
50
51
52
53

54 118 Three rats per group were sacrificed at 0, 4, 7, 14, and 28 days after PA
55 119 injection. After the rats were anesthetized with Pentobarbital sodium (100 mg/kg,
56
57
58
59
60

1
2
3
4
5 120 Dainippon Sumitomo Pharma, Osaka, Japan), they were perfused via the
6
7 121 abdominal aorta with a PLP fixative buffer (4 % paraformaldehyde in 0.1 M lysine).
8
9 122 After perfusional fixation, the kidneys were removed and processed for
10
11 123 immunofluorescence and immunoelectron microscopy. Tissue slices were filled in
12
13 124 Tissue-Tek O.C.T. compound (Sakura Finetek, USA), frozen in liquid nitrogen, and
14
15 125 then stored at -80°C prior to immunofluorescence.
16
17
18
19

20 127 ***Human Tissue Samples***

21
22 128 For specimens of human IgA nephritis, tissue samples were obtained from
23
24 129 the samples of diagnostic renal biopsies performed at Juntendo University Hospital
25
26 130 with the permission of the Ethics Committee on Human Research of Juntendo
27
28 131 University Faculty of Medicine. We investigated the samples from four groups of
29
30 132 four patients, IgAN-good, IgAN-relatively-good (IgAN-r-good), IgAN-relatively-poor
31
32 133 (IgAN-r-poor), IgAN-poor, who had IgA nephropathy diagnosed according to the
33
34 134 second guideline of IgA nephropathy (16). As control human samples, we used
35
36 135 biopsy samples from patients with minor glomerular abnormalities (N = 4).
37
38
39
40

41 137 ***Immunofluorescence***

42
43 138 For the immunofluorescent staining of rat kidneys, $4\ \mu\text{m}$ thick sections on
44
45 139 sialan-coated slide glass were washed in PBS and incubated with a blocking
46
47 140 solution. A double immunofluorescent staining for podocin and synpo was then
48
49 141 performed and the secondary antibodies were incubated.
50
51

52 142 Human kidney biopsy specimens were stored at -80°C for
53
54 143 immunofluorescence. The $4\ \mu\text{m}$ thick sections were fixed with cold acetone for 5
55
56 144 min, washed with PBS, incubated with a blocking solution, and then a double
57
58
59
60

1
2
3
4
5 145 immunofluorescent staining for podocin and synpo was performed using the same
6
7 146 methodology as with the PAN rats. These sections were photographed under a
8
9 147 confocal laser microscope (Olympus FV1000, Tokyo, Japan).

10
11 148 To examine the podocin gap, or the staining gap between the area of
12
13 149 podocin and synpo, at least 50 mid-sections of podocin and synpo areas were
14
15 150 carefully measured using a digitizer KS-400 Imaging System as described
16
17 151 previously (17) and the podocin gap was calculated using the following formula:
18
19 152 podocin gap (%) = (podocin fluorescent staining area – synpo fluorescent staining
20
21 153 area) / area of each glomerulus × 100.
22
23
24
25

26 155 ***Immunoelectron microscopy***

27
28 156 Animals were perfused with physiological saline and subsequently with a
29
30 157 PLP fixative. The perfused kidneys were cut into small pieces, and immersed in the
31
32 158 same fixative for 30 min. The samples were dehydrated with a graded series of
33
34 159 ethanol and embedded in an LR-white resin (London Resin, Berkshire, UK) (18).
35
36 160 Ultrathin gold sections of the LR-white-resin-embedded samples were produced
37
38 161 with a diamond knife and transferred to nickel grids (150 mesh) that had been
39
40 162 coated with a Formvar membrane. After blocking with a 1 % normal goat serum in
41
42 163 PBS (pH 7.4), the sections were incubated overnight with the anti-podocin
43
44 164 antiserum (1:50) diluted with 1 % BSA in PBS at 4 °C for 12 hours. Subsequently
45
46 165 they were incubated with colloidal-gold-conjugated secondary antibodies (BBI,
47
48 166 Cardiff, UK) diluted 1:100 with 1 % BSA in PBS for one hour at room temperature,
49
50 167 contrasted with 4 % uranyl acetate for 5 min, and observed with an H7100
51
52 168 transmission electron microscope (Hitachi High-Technologies, Tokyo, Japan). The
53
54 169 primary antibodies were omitted from the incubation solution as a negative control,
55
56
57
58
59
60

1
2
3
4
5 170 and no non-specific staining of the secondary antibody was found in the kidney
6
7 171 sections.

8
9 172 To confirm the alteration of localization of podocin in PAN rats, pictures
10
11 173 from at least 15 podocyte cell bodies from each day were taken after an
12
13 174 immunoelectron microscopic study. The immunogold podocin particles in the
14
15 175 podocyte cell body were counted.

16
17 176 To examine the localization of podocin in human IgAN, tissues were taken
18
19 177 with needle biopsy. Small cortical pieces were incubated in a PLP fixative buffer
20
21 178 for a few hours and embedded in LR-white, the same as with the rat kidney tissues.
22
23 179

24 25 26 180 ***Statistical analysis***

27
28 181 All values are means +SEM. Statistical significance (defined as $P < 0.05$)
29
30 182 was evaluated using Stat View followed by the Fisher's paired least significant
31
32 183 difference t test.
33
34 184

35
36
37 185 [Results]

38 39 186 *PAN rats showed significant proteinuria*

40
41 187 A single intraperitoneal injection of PAN produces overt proteinuria on
42
43 188 days 4 to 28 (Fig. 1). We compared the levels of proteinuria at each time point from
44
45 189 day 0. All time points, or days 4, 7, 14, and 28, showed significant proteinuria ($p <$
46
47 190 0.001). On day 28, the levels of proteinuria had decreased from the peak levels
48
49 191 observed on day 14.
50

51
52 192
53
54 193 *PAN rats showed a difference in the staining of podocin and synpo on days 7 and*

55
56 194 *14*
57
58
59
60

1
2
3
4
5 195 Although on days 4 and 7 the expression of podocin and synpo were
6
7 196 decreased, they were recovered on days 14 and 28 (Fig. 2a-e). The expression of
8
9 197 podocin seemed to follow a linear pattern (similar to the glomerular basement
10
11 198 membrane: GBM type) on days 4 and 7, and a podocyte cell body pattern on days
12
13 199 14 and 28. On the other hand, the linear staining of synpo did not change during
14
15 200 the period from day 4 to 28. On day 0, the staining pattern of podocin and synpo
16
17 201 were almost matched (Fig. 2a). On days 7–14, the area of podocin seemed to be
18
19 202 translocated to the cell body area from the foot process area, however synpo stayed
20
21 203 in the foot process area (Fig. 2c, d).

22
23
24 204 On day 28 their merged area was relocated to the foot process area (Fig.
25
26 205 2e). To confirm the difference of the podocin-synpo area, we calculated the podocin
27
28 206 gap (ref. materials and methods) with the use of computer software by subtracting
29
30 207 the synpo area from the podocin area, and dividing the total by the glomerulus
31
32 208 area (Fig. 2f). On days 7–14 the podocin gap was significantly increased ($p < 0.05$)
33
34 209 and on day 28 the area returned to the same size as measured on day 0.

35
36
37 210

38 39 211 *Podocin was translocated to the cytoplasm of PAN rats at day 14*

40
41 212 In the immunoelectron microscopy of PAN rats, immunoreactive podocin
42
43 213 was recognized by gold particles (Fig. 3a, b, c: low magnification $\times 8000$ – 20000 , 3a',
44
45 214 b', c': high magnification $\times 10000$ – 50000). On day 0, podocin was recognized at the
46
47 215 slit diaphragm insertion sites of foot processes (Fig. 3a, day 0). On day 7, the
48
49 216 structure of the slit diaphragm was destroyed and the podocin was translocated to
50
51 217 the cell bodies of the podocytes (Fig. 3b, day 7). On day 14, through staining,
52
53 218 podocin was seen in the vesicular structures in the cell bodies of podocytes (Fig. 3c,
54
55 219 day 14). This data indicates that the podocin was translocated to the cell body,
56
57
58
59
60

1
2
3
4
5 220 likely by endocytosis.

6
7 221 By counting the number of gold particles in the cytoplasm of the podocytes, we
8
9 222 could detect significantly more podocin in the cytoplasm on days 7 and 14, as
10
11 223 compared to day 0 (Fig. 3d, $p < 0.05$).

12
13
14 224

15
16 225 *The podocin gap was significantly increased in IgAN-poor prognosis specimens*

17
18 226 Each of the four IgAN groups consisted of four samples that were stained
19
20 227 with podocin and synpo (Fig. 4a-e). In the IgAN-good group, the podocin and synpo
21
22 228 stained areas were consistently similar to day 0 in PAN rats (Fig. 4b, IgAN-good).
23
24 229 In the IgAN-r-good group the level of expression was decreased, but both of them
25
26 230 were merged completely (Fig. 4c, IgAN-r-good). In the IgAN-r-poor group, there
27
28 231 was no evident change from the IgAN-good group (Fig. 4d, IgAN-r-poor).

29
30 232 Surprisingly, in the IgAN-poor group, podocin was stained in the cell bodies of
31
32 233 podocytes and there was a clear difference in the staining pattern between podocin
33
34 234 and synpo. This result suggests the translocation of podocin to the cytoplasm. We
35
36 235 also measured the podocin gap in each human biopsy sample from IgAN (Fig. 4f)
37
38 236 using the previously mentioned software. The podocin gap was not altered in the
39
40 237 IgAN-r-good and IgAN-r-poor groups when compared to the control group. However,
41
42 238 in the IgAN-poor group it was significantly increased ($p < 0.05$) when compared to
43
44 239 the area of the IgAN-r-good group, indicating that podocin translocated to the cell
45
46 240 bodies of podocytes.

47
48
49 241

50
51
52 242 *Podocin was translocated to the cytoplasm in IgAN poor prognosis specimens*

53
54 243 Next we performed immunoelectron microscopy using an anti-podocin
55
56 244 antibody in kidney biopsy specimens of minor glomerular injury and IgAN-poor
57
58
59
60

1
2
3
4
5 245 specimens (Fig. 5a-c). Podocin was located in the SD area of the control specimen.

6
7 246 On the other hand, in the IgAN-poor biopsy specimens, the structure of the foot

8
9 247 processes was destroyed and podocin was translocated to cytoplasm area (Fig. 5b, c,

10
11 248 IgAN-poor).

12
13
14 249

15
16 250 *Podocin was translocated to the cytoplasm by the endocytosis pathway*

17
18 251 As we mentioned above before, at day14 of PAN rats podocin was

19
20 252 translocated to the cell body area from foot processes. To check this translocation

21
22 253 mechanism, we stained PAN rats specimens at day 14 with podocin and Rab5

23
24 254 (early endosome marker)(Fig. 6a, b). Several podocytes were merged with Rab5 and

25
26 255 this result indicated that podocin was translocated to cytoplasm by the endocytosis

27
28 256 pathway.

29
30
31 257

32
33 258 *Podocin was not translocated to the cytoplasm in minimal change disease*

34
35 259 We evaluated the podocin gap in human minimal change disease (MCD)

36
37 260 biopsy specimens. Podocin and synpo merged clearly and no podocin gap could be

38
39 261 detected in MCD (Fig.7).

40
41
42
43
44
45
46
47
48
49
50
51
52
53
54
55
56
57
58
59
60

1
2
3
4
5 262 [Discussion]
6

7 263 In this paper, we demonstrated that podocin was translocated from the SD
8
9 264 area to the cytoplasm area by the endocytosis pathway in PAN rats and in the
10
11 265 IgAN-poor prognosis group. We defined the podocin gap as follows: the difference in
12
13 266 the staining pattern between podocin and synpo, which are foot processes proteins.
14
15 267 Podocin is especially prevalent in the SD, but synpo is located beside actin bundles
16
17 268 in the foot processes (21). As we demonstrated before, synpo is a critical protein for
18
19 269 podocytes and for organizing their structure (22). In the absence of synpo, the
20
21 270 podocytes lose essential stress fibers and their cell bodies shrink so as to resemble
22
23 271 a fibroblast. On the other hand, SD proteins were naturally translocated from SD
24
25 272 to the cytoplasm, and keep its structure (23). Within a diseased condition, the
26
27 273 endocytosis system of SD proteins may become damaged and the damage may
28
29 274 accelerate podocyte injury. Thus, we hypothesize that the difference of localization
30
31 275 between podocin and synpo may occur during podocyte injury. During proteinuria
32
33 276 conditions, the difference between the localization of podocin and synpo was
34
35 277 significantly more evident than during normal conditions. To focus on the podocin
36
37 278 gap, we checked the localization of podocin, and therefore we also demonstrated
38
39 279 that podocin was translocated to the cytoplasmic area with immune-electron
40
41 280 microscopy. Although podocin was traslocated to the cytoplasm, it does not
42
43 281 correlate to the level of proteinuria. Actually the podocin gap was not found in
44
45 282 either MCD, IgAN-r-good or IgAN-r-poor specimens. We estimated that the
46
47 283 translocation of podocin happened in severe podocyte injury.
48
49
50

51 284 Soda *et al.* reported that double knocked-out dynamin-1 and -2 mice,
52
53 285 synaptojanin knocked-out mice, and triple endophilin-1, -2, and -3 knocked-out mice
54
55 286 showed significant proteinuria and foot process effacement (24). They further
56
57
58
59
60

1
2
3
4
5 287 demonstrated that synaptojanin and endophilin, which are functional partners of
6
7 288 dynamin in synaptic vesicle endocytosis at neural synapses, were critically
8
9 289 implicated in the development of the permeability barrier of kidneys. This paper
10
11 290 indicated that the system of endocytosis in the podocytes is a critical phenomenon,
12
13 291 and that it is tightly connected to proteinuria and foot process effacement further
14
15 292 worsening the podocyte injury (these knocked-out mice displayed a lethal kidney
16
17 293 failure).

18
19
20 294 Recent evidence suggests that endocytosis may play a vital role in the
21
22 295 internalization and recycling of nephrin (25). Phosphorylation (26) and the
23
24 296 stimulation of high glucose (25) may initiate nephrin endocytosis and depends on
25
26 297 CIN/RukL, the homologue of CD2AP (27). Focusing on endocytosis, Qin *et al.*
27
28 298 demonstrated that a raft-mediated endocytic pathway internalizes nephrin (28),
29
30 299 and Godel *et al.* demonstrated that the trafficking of podocin is dependent on the
31
32 300 raft-mediated, non-conventional endocytic pathway (29). This seems to be
33
34 301 consistent with the suggestion for endocytic trafficking of other prohibitin-domain
35
36 302 proteins (30). Intriguingly, the podocin-related protein flotillin-1 defines a clathrin-
37
38 303 independent endocytic pathway (31), which could lead to the hypothesis that
39
40 304 podocin not only assembles members of the slit diaphragm but also orchestrates its
41
42 305 internalization via a self-defined pathway (29). In this study, we demonstrated
43
44 306 that podocin merged with Rab5 in PAN rats at day 14. At the same time the
45
46 307 podocin gap was significantly elevated, indicating that podocin was translocated to
47
48 308 the cytoplasm by the endocytosis pathway. Because Rab5 is a typical CME marker,
49
50 309 it shows evidence that podocin was interacts with the CME pathway.

51
52
53 310 The Wiggins group demonstrated that a single dose of PA caused
54
55 311 podocytes depletion that results in minor glomerular sclerosis (32). As a podocyte
56
57
58
59
60

1
2
3
4
5 312 injury model we used PAN rats with a single peritoneal PA injection with the same
6
7 313 methods of Wiggis' group. For our model of podocyte injury, we used PAN rats
8
9 314 prepared with a single peritoneal PA injection, just as Wiggis' group used for their
10
11 315 experiment. PA induces oxidant injury in cells via the xanthine oxidase pathway,
12
13 316 and it was used as a similar model of MCD and focal segmental nephron sclerosis
14
15 317 in human (33). We evaluated PAN rats samples, which showed podocytes
16
17 318 detachment and glomerular sclerosis. Clinically, MCD does not show such podocyte
18
19 319 change without foot process effacement (FPE), so we used this model as a
20
21 320 podocytes injury model. We also tried to stain the podocin gap in human MCD,
22
23 321 however, there was no difference in the podocin and synpo staining (Fig. 7).
24
25

26 322 Recently, two papers demonstrated that FPE has been interpreted as a
27
28 323 protective response of podocytes in danger of detachment (34,35). This FPE is
29
30 324 observed typically in MCD and in other glomerulonephritis. Similarly, PAN rats
31
32 325 and IgAN patients also show these pathological findings. The point is that the
33
34 326 podocin gap was observed only on PAN day 7, 14 and IgAN-poor. These
35
36 327 pathological findings show severe glomerular damage and podocytes injury.
37
38 328 Compared to FPE, the podocin gap was only seen in severe conditions, we thought
39
40 329 it could be a predictive factor to assess the IgAN.
41
42

43 330 IgAN is the most common primary glomerulonephritis. An often insidious
44
45 331 progression to end-stage kidney disease in 25–40 % of cases is accompanied by the
46
47 332 development of glomerulosclerosis (36). It is characterized by the mesangial
48
49 333 deposition of IgA, associated with mesangial cell proliferation and mesangial
50
51 334 matrix expansion. In addition to these common histologic abnormalities, other
52
53 335 glomerular abnormalities, such as segmental sclerosis, crescent formation, and
54
55 336 adhesion to the bowman capsules, are detected. Other indicators, such as the
56
57
58
59
60

1
2
3
4
5 337 number of podocytes per glomerulus might serve as a parameter of podocyte injury
6
7 338 and provide prognostic information for patients with IgAN (37). Lemley et al.
8
9 339 reported that podocytopenia is associated with increasing disease severity in IgAN
10
11 340 (38). The clinical course of IgAN is variable. The prevalence of clinically silent
12
13 341 IgAN may be surprising high; in a Japanese study, 16 % of donor kidneys had
14
15 342 glomerular IgA deposits and nearly 2 % exhibited mesangioproliferative changes
16
17 343 with C3 deposits characteristic of IgAN (39). Mesangial IgA is exclusively of the
18
19 344 IgA1 subclass and is deficient in galactose (40). Besides these findings, the
20
21 345 proceeding mechanisms of IgAN are still obscure. Therefore, we focused on the
22
23 346 difference in pathological characterizations of IgAN. On this basis, we divided
24
25 347 IgAN samples into 4 categories, following the indicators of Japan Committee of
26
27 348 IgAN 2002, and assessed each specimen. Only the poor prognosis specimens
28
29 349 showed a significant difference in the podocin gap, and this showed a translocation
30
31 350 of podocin to cytoplasm by endocytosis. Based on these results, we hypothesize that
32
33 351 podocin traffic may lead to severe podocyte injury or may happen in severely
34
35 352 injured podocytes. With these results, we postulate that podocin traffic may also
36
37 353 predict the prognosis of an IgAN disease course.

38
39
40
41 354 When evaluating IgAN, the patient's samples are very important for
42
43 355 estimating their prognosis, however at present we do not have a specific staining
44
45 356 reference. If endocytosis is more fully understood, the movement of some proteins
46
47 357 may be the key to knowing the turning point between reversible change and
48
49 358 irreversible change.

50
51
52 359 In the future, the role of podocin traffic may help shed light on the
53
54 360 mechanism of podocyte injury and indicate a medical approach to prevent the
55
56 361 advancement of the disease course.
57
58
59
60

1
2
3
4
5 362 [Acknowledgement]
6

7 363 **Acknowledgments**
8

9 364 We thank Ms. Terumi Shibata, Ms. Kaori Takahashi, Mr. Junichi
10
11 365 Nakamoto, and Mr. Mitsutaka Yoshida, of Juntendo University Graduate School of
12
13 366 Medicine, Tokyo, Japan, for their excellent technical assistance. This work was
14
15 367 supported by a research assistant grant from the Research Institute for Diseases of
16
17 368 Old Age to J. A. O. T., by a Grant-in-Aid for Scientific Research (C): (23591201) and
18
19 369 a Grant-in-Aid for Challenging Exploratory Research (26670431) to K.A., by a
20
21 370 Grant-in-Aid for Young Scientists (B): (24790856) to M. A-T., and by a Grant-in-Aid
22
23 371 for Young Scientists (B): (23790956) to T. H..
24
25
26
27
28
29
30
31
32
33
34
35
36
37
38
39
40
41
42
43
44
45
46
47
48
49
50
51
52
53
54
55
56
57
58
59
60

372

1 [References]

2 1. Kestila M, Lenkkeri U, Mannikko M, Lamerdin J, McCready P, Putaala H, et al.

3 Positionally cloned gene for a novel glomerular protein--nephrin--is mutated in

4 congenital nephrotic syndrome. *Mol Cell*. 1998 Mar;1(4):575-82.

5 2. Ruotsalainen V, Ljungberg P, Wartiovaara J, Lenkkeri U, Kestila M, Jalanko H,

6 et al. Nephrin is specifically located at the slit diaphragm of glomerular podocytes.

7 *Proc Natl Acad Sci U S A*. 1999 Jul 6;96(14):7962-7.

8 3. Boute N, Gribouval O, Roselli S, Benessy F, Lee H, Fuchshuber A, et al. NPHS2,

9 encoding the glomerular protein podocin, is mutated in autosomal recessive

10 steroid-resistant nephrotic syndrome. *Nat Genet*. 2000 Apr;24(4):349-54.

11 4. Tryggvason K, Patrakka J, Wartiovaara J. Hereditary proteinuria syndromes and

12 mechanisms of proteinuria. *N Engl J Med*. 2006 Mar 30;354(13):1387-401.

13 5. Huber TB, Simons M, Hartleben B, Sernetz L, Schmidts M, Gundlach E, et al.

14 Molecular basis of the functional podocin-nephrin complex: Mutations in the NPHS2

15 gene disrupt nephrin targeting to lipid raft microdomains. *Hum Mol Genet*. 2003

16 Dec 15;12(24):3397-405.

17 6. Schwarz K, Simons M, Reiser J, Saleem MA, Faul C, Kriz W, et al. Podocin, a

18 raft-associated component of the glomerular slit diaphragm, interacts with CD2AP

19 and nephrin. *J Clin Invest*. 2001 Dec;108(11):1621-9.

1
2
3
4
5
6
7
8
9
10
11
12
13
14
15
16
17
18
19
20
21
22
23
24
25
26
27
28
29
30
31
32
33
34
35
36
37
38
39
40
41
42
43
44
45
46
47
48
49
50
51
52
53
54
55
56
57
58
59
60

- 1
2
3
4
5
6 20 7. Roselli S, Moutkine I, Gribouval O, Benmerah A, Antignac C. Plasma membrane
7
8 21 targeting of podocin through the classical exocytic pathway: Effect of NPHS2
9
10 22 mutations. *Traffic*. 2004 Jan;5(1):37-44.
11
12
13
14 23 8. Le Roy C, Wrana JL. Clathrin- and non-clathrin-mediated endocytic regulation of
15
16 24 cell signalling. *Nat Rev Mol Cell Biol*. 2005 Feb;6(2):112-26.
17
18
19
20 25 9. Mayor S, Pagano RE. Pathways of clathrin-independent endocytosis. *Nat Rev Mol*
21
22 26 *Cell Biol*. 2007 Aug;8(8):603-12.
23
24
25
26 27 10. Shono A, Tsukaguchi H, Yaoita E, Nameta M, Kurihara H, Qin XS, et al. Podocin
27
28 28 participates in the assembly of tight junctions between foot processes in nephrotic
29
30 29 podocytes. *J Am Soc Nephrol*. 2007 Sep;18(9):2525-33.
31
32
33
34 30 11. Asanuma K, Tanida I, Shirato I, Ueno T, Takahara H, Nishitani T, et al.
35
36 31 MAP-LC3, a promising autophagosomal marker, is processed during the
37
38 32 differentiation and recovery of podocytes from PAN nephrosis. *FASEB J*. 2003
39
40 41 Jun;17(9):1165-7.
42
43
44
45 34 12. Diamond JR, Bonventre JV, Karnovsky MJ. A role for oxygen free radicals in
46
47 35 aminonucleoside nephrosis. *Kidney Int*. 1986 Feb;29(2):478-83.
48
49
50
51 36 13. Nosaka K, Takahashi T, Nishi T, Imaki H, Suzuki T, Suzuki K, et al. An
52
53 37 adenosine deaminase inhibitor prevents puromycin aminonucleoside nephrotoxicity.
54
55
56 38 *Free Radic Biol Med*. 1997;22(4):597-605.
57
58
59
60

- 1
2
3
4
5
6 39 14. Inokuchi S, Shirato I, Kobayashi N, Koide H, Tomino Y, Sakai T. Re-evaluation
7
8 40 of foot process effacement in acute puromycin aminonucleoside nephrosis. *Kidney*
9
10 41 *Int.* 1996 Oct;50(4):1278-87.
12
13
14 42 15. Kihara I, Yatoita E, Kawasaki K, Yamamoto T. Limitations of podocyte
15
16 43 adaptation for glomerular injury in puromycin aminonucleoside nephrosis. *Pathol*
17
18 44 *Int.* 1995 Sep;45(9):625-34.
20
21
22 45 16. Tomino Y, Sakai H, Special Study Group (IgA Nephropathy) on Progressive
23
24 46 Glomerular Disease. Clinical guidelines for immunoglobulin A (IgA) nephropathy in
25
26 47 japan, second version. *Clin Exp Nephrol.* 2003 Jun;7(2):93-7.
27
28
29
30
31 48 17. Tanimoto M, Fan Q, Gohda T, Shike T, Makita Y, Tomino Y. Effect of
32
33 49 pioglitazone on the early stage of type 2 diabetic nephropathy in KK/ta mice.
34
35 50 *Metabolism.* 2004 Nov;53(11):1473-9.
36
37
38
39 51 18. Ichimura K, Kurihara H, Sakai T. Beta-cytoplasmic actin localization in
40
41 52 vertebrate glomerular podocytes. *Arch Histol Cytol.* 2009;72(3):165-74.
42
43
44
45 53 19. Shankland SJ. The podocyte's response to injury: Role in proteinuria and
46
47 54 glomerulosclerosis. *Kidney Int.* 2006 Jun;69(12):2131-47.
48
49
50
51 55 20. Kim YH, Goyal M, Kurnit D, Wharram B, Wiggins J, Holzman L, et al. Podocyte
52
53 56 depletion and glomerulosclerosis have a direct relationship in the PAN-treated rat.
54
55
56 57 *Kidney Int.* 2001 Sep;60(3):957-68.
57
58
59
60

- 1
2
3
4
5
6 58 21. Shirato I, Sakai T, Kimura K, Tomino Y, Krit W. Cytoskeletal changes in
7
8 59 Podocytes associated with foot process effacement in masugi nephritis. *Am J. Pathol.*
9
10 60 1996 April;148(4):1283-1296
11
12
13
14 61 22. Asanuma K, Yanagida-Asanuma E, Faul C, Tomino Y, Kim K, Mundel P.
15
16 62 Synaptopodin orchestrates actin organization and cell motility via regulation of
17
18 63 RhoA signalling. *Nat Cell Biol.* 2006 May;8(5):485-91.
19
20
21
22 64 23. Soda K, Ishibe S. The function of endocytosis in podocytes. *Curr Opin Nephrol*
23
24 65 *Hypertens.* 2013 Jul;22(4):432-8.
25
26
27
28 66 24. Soda K, Balkin DM, Ferguson SM, Paradise S, Milosevic I, Giovedi S, et al. Role
29
30 67 of dynamin, synaptojanin, and endophilin in podocyte foot processes. *J Clin Invest.*
31
32 68 2012 Dec 3;122(12):4401-11.
33
34
35
36
37 69 25. Tossidou I, Teng B, Menne J, Shushakova N, Park JK, Becker JU, et al.
38
39 70 Podocytic PKC-alpha is regulated in murine and human diabetes and mediates
40
41 71 nephrin endocytosis. *PLoS One.* 2010 Apr 16;5(4):e10185.
42
43
44
45 72 26. Quack I, Rump LC, Gerke P, Walther I, Vinke T, Vonend O, et al. Beta-Arrestin2
46
47 73 mediates nephrin endocytosis and impairs slit diaphragm integrity. *Proc Natl Acad*
48
49 74 *Sci U S A.* 2006 Sep 19;103(38):14110-5.
50
51
52
53 75 27. Tossidou I, Niedenthal R, Klaus M, Teng B, Worthmann K, King BL, et al.
54
55 76 CD2AP regulates SUMOylation of CIN85 in podocytes. *Mol Cell Biol.* 2012
56
57
58
59
60

- 1
2
3
4
5
6 77 Mar;32(6):1068-79.
7
8
9
10 78 28. Qin XS, Tsukaguchi H, Shono A, Yamamoto A, Kurihara H, Doi T.
11
12 79 Phosphorylation of nephrin triggers its internalization by raft-mediated endocytosis.
13
14 80 J Am Soc Nephrol. 2009 Dec;20(12):2534-45.
15
16
17
18 81 29. Godel M, Ostendorf BN, Baumer J, Weber K, Huber TB. A novel domain
19
20 82 regulating degradation of the glomerular slit diaphragm protein podocin in cell
21
22 83 culture systems. PLoS One. 2013;8(2):e57078.
23
24
25
26 84 30. Langhorst MF, Reuter A, Stuermer CA. Scaffolding microdomains and beyond:
27
28 85 The function of reggie/flotillin proteins. Cell Mol Life Sci. 2005
29
30 86 Oct;62(19-20):2228-40.
31
32
33
34 87 31. Glebov OO, Bright NA, Nichols BJ. Flotillin-1 defines a clathrin-independent
35
36 88 endocytic pathway in mammalian cells. Nat Cell Biol. 2006 Jan;8(1):46-54.
37
38
39
40 89 32. Kim YH, Goyal M, Wharram B, Wiggins J, Kershaw D, Wiggins R. GLEPP1
41
42 90 receptor tyrosine phosphatase (Ptpro) in rat PAN nephrosis. A marker of acute
43
44 91 podocyte injury. Nephron. 2002 Apr;90(4):471-6.
45
46
47
48
49 92 33. Seckin I, Uzunalan M, Pekpak M, Kokturk S, Sonmez H, Oztürk Z, et al.
50
51 93 Experimentally induced puromycin aminonucleoside nephrosis (PAN) in rats:
52
53 94 evaluation of angiogenic protein platelet-derived endothelial cell growth factor
54
55 95 (PD-ECGF) expression in glomeruli. J Biomed Sci. 2012 Feb 16;19-24.
56
57
58
59
60

- 1
2
3
4
5
6 96 34. Kriz W, Shirato I, Nagata M, LeHir M, Lemley KV. The podocyte's response to
7
8 97 stress: the enigma of foot process effacement. *Am J Physiol Renal Physiol*. 2013 Feb
9
10 98 15:304(4):F333-47.
11
12
13
14 99 35. Kriz W, Lemley KV. A Potential Role for Mechanical Forces in the Detachment
15
16 100 of Podocytes and the Progression of CKD. *J Am Soc Nephrol*. 2014 Jul; 24.
17
18
19
20 101 36. Rychlik I, Andrassy K, Waldherr R, Zuna I, Tesar V, Jancova E, et al. Clinical
21
22 102 features and natural history of IgA nephropathy. *Ann Med Interne (Paris)*. 1999
23
24 103 Feb;150(2):117-26.
25
26
27
28 104 37. Hishiki T, Shirato I, Takahashi Y, Funabiki K, Horikoshi S, Tomino Y. Podocyte
29
30 105 injury predicts prognosis in patients with iga nephropathy using a small amount of
31
32 106 renal biopsy tissue. *Kidney Blood Press Res*. 2001;24(2):99-104.
33
34
35
36
37 107 38. Lemley KV, Lafayette RA, Safai M, Derby G, Blouch K, Squarer A, et al.
38
39 108 Podocytopenia and disease severity in IgA nephropathy. *Kidney Int*. 2002
40
41 109 Apr;61(4):1475-85.
42
43
44
45 110 39. Suzuki K, Honda K, Tanabe K, Toma H, Nihei H, Yamaguchi Y. Incidence of
46
47 111 latent mesangial IgA deposition in renal allograft donors in japan. *Kidney Int*. 2003
48
49 112 Jun;63(6):2286-94.
50
51
52
53 113 40. Suzuki H, Kiryluk K, Novak J, Moldoveanu Z, Herr AB, Renfrow MB, et al. The
54
55 114 pathophysiology of IgA nephropathy. *J Am Soc Nephrol*. 2011 Oct;22(10):1795-803.
56
57
58
59
60

1 [Figure Legends]

2 **Fig. 1: Puromycin Aminonucleoside (PA) Nephrosis (PAN) rats showed significant**
3 **proteinuria.**

4 Urinary protein was measured before and after the peritoneal injection of PA (15
5 mg/kg) to rats ($N \geq 4$). On days 4, 7, 14, and 28 urinary protein was significantly
6 increased ($p < 0.001$) (Mean \pm SE).

7
8 **Fig. 2a-e: Double fluorescence of podocin (green), synaptopodin (synpo) (red), and**
9 **merged (yellow) in PAN rats.**

10 On day 4 the expression of podocin was decreased, and the synpo area seemed larger
11 than that of podocin, but on days 7 and 14 the pattern of podocin staining had
12 changed from a linear to cytoplasmic pattern. On day 28 the area of both stainings
13 were similar to control conditions (day 0). Scale bar: 50 μ m (a-e)

14
15 **Fig. 2f: Changes in the discrepancy staining area with podocin and synpo for each**
16 **time course.**

17 We measured the podocin gap, the difference in the fluorescence staining area
18 between podocin and synpo for each time point specimen for over 50 glomeruli using
19 specific computer software (the mathematical formula is above this legend). KS400
20 software. ref. material and method). On days 7 and 14 the gap was significantly
21 increased ($n \geq 50$) ($p < 0.05$) (Mean \pm SE).

22
23 **Fig. 3a-c: Immunoelectron microscopy of podocin in PAN rats.**

24 Podocin moved from the slit diaphragm area to the cytoplasmic area as form of

1
2
3
4
5 25 vesicles at day 14 in the podocytes. Scale bar: 50nm (a-c, a'-c')

6
7 26 *The left-side figure shows low magnification pictures ($\times 8000$ – 20000) and the*

8
9 27 *right-side shows high magnification pictures ($\times 10000$ – 50000).*

10
11
12 28

13
14 29 **Fig. 3d: Podocin significantly moved to the cytoplasm of podocytes on days 7 and 14**

15
16 30 **in PAN rats.**

17
18 31 The number of gold particles (podocin) was calculated in the cytoplasmic area of

19
20 32 podocytes. On days 7 and 14 podocin was significantly increased in the cytoplasmic

21
22 33 area in podocytes ($n \geq 15$) ($p < 0.05$) (Mean \pm SE).

23
24
25 34

26
27 35 **Fig. 4a-e: Double fluorescence of podocin (green), synpo (red), and merged (yellow) in**

28
29 36 **IgA Nephropathy.**

30
31 37 In IgAN-good, -r-good, and -r-poor specimens, the staining area of podocin and synpo

32
33 38 were almost the same, but the IgAN-poor podocin area (not merged with synpo,

34
35 39 green) was larger than that of the other groups, and the staining pattern had

36
37 40 changed from a linear type to cell body type. Scale bar: 50 μ m (a-e)

38
39
40 41

41
42 42 **Fig. 4f: The changes in the discrepancy staining area with podocin and synpo in each**

43
44 43 **prognosis categories of IgAN.**

45
46 44 We measured the podocin gap (refer to Fig. 2f). In IgAN-r-good specimens, the gap

47
48 45 was decreased as compared with that of the control, but interestingly in the

49
50 46 IgAN-poor group the gap was significantly increased ($p < 0.05$) compared with that

51
52 47 of IgAN-r-good.

53
54
55 48 control specimens, i.e. minor glomerular abnormality ($n \geq 4$) (Mean \pm SE).

56
57
58
59
60

1
2
3
4
5 49
6

7 **Fig. 5a-c: Immunoelectron microscopy of podocin in the control and IgAN-poor**
8 **group.**
9

10
11 Podocin was translocated from the slit diaphragm area to the cytoplasmic area in
12 the IgAN-poor group. Scale bar: 500nm (a, a', c'), 2 μ m (b, b', c)

13
14
15 Normal glomerulus: minor glomerular abnormalities

16
17
18 *The left-side figure shows low magnification pictures ($\times 8000$) and the right-side*
19
20 *shows high magnification pictures ($\times 30000$).*
21

22 57

23
24 **Fig.6a, b: Podocin and Rab5 merged in samples from day 14 PAN rats.**
25

26 We performed double staining of podocin and Rab, which is a specific early
27
28 endosome marker, in day 14 PAN rats specimens, and detected several locations
29
30 were podocin clearly merged with Rab5 (arrow). This suggests podocin translocation
31
32 to the cytoplasm by endocytosis. Scale bar: 50 μ m (a, b)
33
34

35 63

36
37 **Fig.7: In human MCD podocin and synpo merged clearly and there was no**
38 **significant podocin gap.**
39

40
41 Evaluation of the podocin gap in human MCD specimens showed that podocin and
42
43 synpo stained the same foot process area. We did not find any evidence of podocin
44
45 translocation. Scale bar: 50 μ m (a)
46
47

48 69
49
50
51
52
53
54
55
56
57
58
59
60

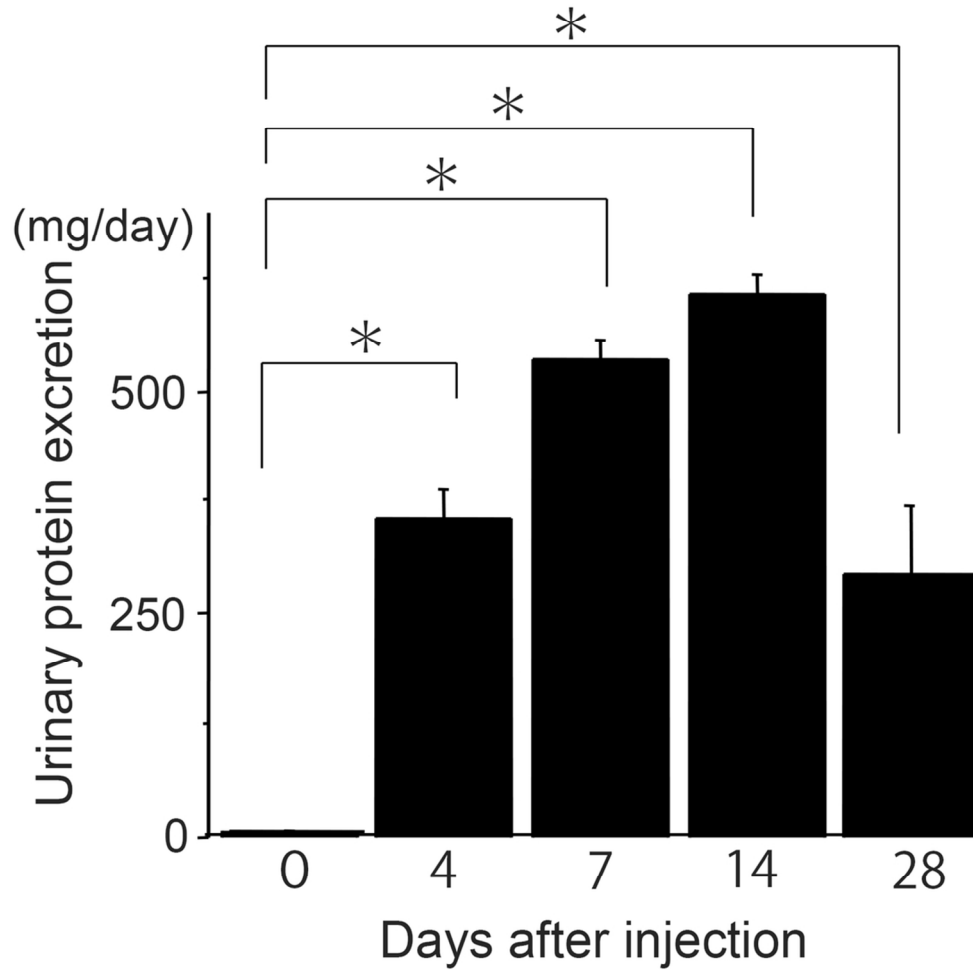


Fig. 1: Puromycin Aminonucleoside (PA) Nephrosis (PAN) rats showed significant proteinuria. Urinary protein was measured before and after the peritoneal injection of PA (15 mg/kg) to rats ($N \geq 4$). On days 4, 7, 14, and 28 urinary protein was significantly increased ($p < 0.001$) (Mean \pm SE).

98x115mm (300 x 300 DPI)

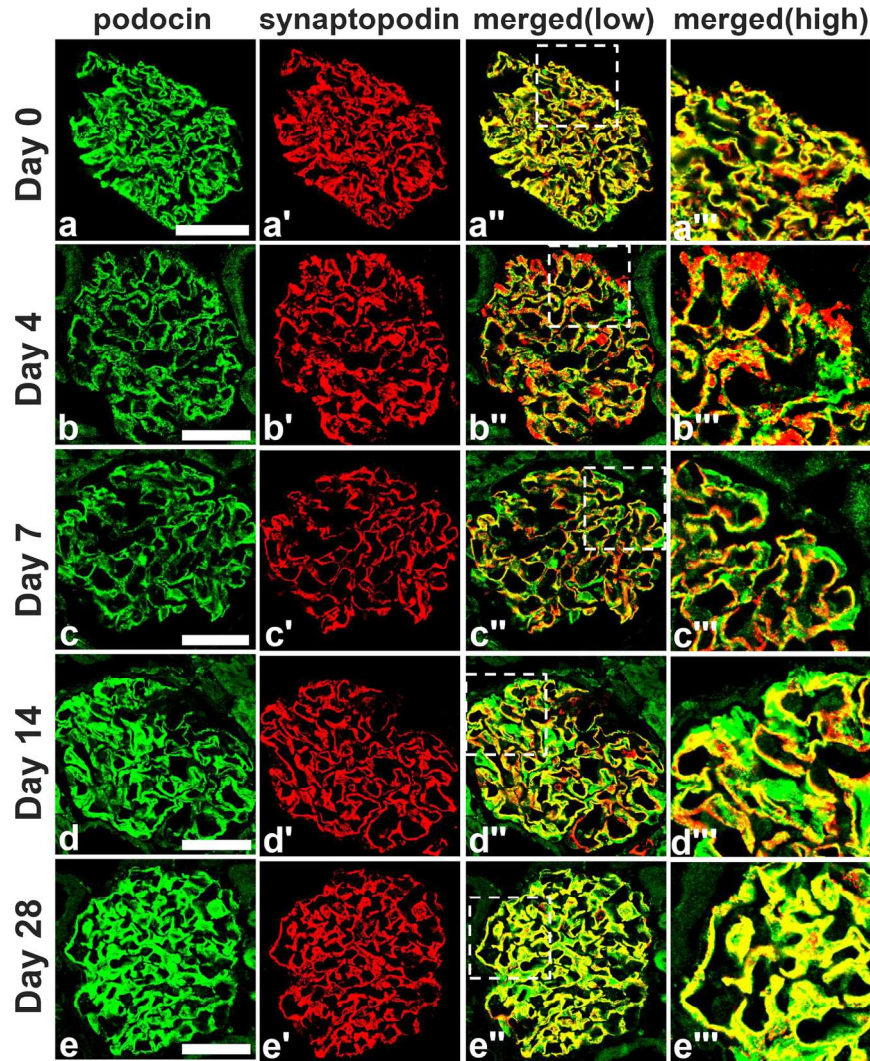
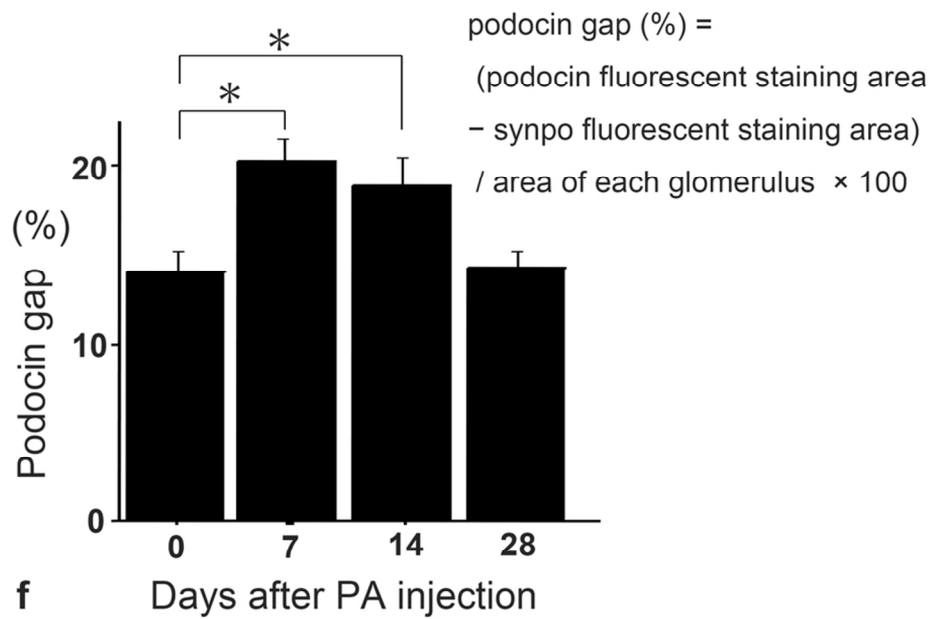


Fig. 2a-e: Double fluorescence of podocin (green), synaptopodin (synpo) (red), and merged (yellow) in PAN rats.

On day 4 the expression of podocin was decreased, and the synpo area seemed larger than that of podocin, but on days 7 and 14 the pattern of podocin staining had changed from a linear to cytoplasmic pattern. On day 28 the area of both stainings were similar to control conditions (day 0). Scale bar: 50 μ m (a-e)

165x212mm (300 x 300 DPI)



29 Fig. 2f: Changes in the discrepancy staining area with podocin and synpo for each time course.
30 We measured the podocin gap, the difference in the fluorescence staining area between podocin and synpo
31 for each time point specimen for over 50 glomeruli using specific computer software (the mathematical
32 formula is above this legend). KS400 soft ware. ref. material and method). On days 7 and 14 the gap was
33 significantly increased ($n \geq 50$) ($p < 0.05$) (Mean \pm SE).

34 83x54mm (300 x 300 DPI)

35
36
37
38
39
40
41
42
43
44
45
46
47
48
49
50
51
52
53
54
55
56
57
58
59
60

1
2
3
4
5
6
7
8
9
10
11
12
13
14
15
16
17
18
19
20
21
22
23
24
25
26
27
28
29
30
31
32
33
34
35
36
37
38
39
40
41
42
43
44
45
46
47
48
49
50
51
52
53
54
55
56
57
58
59
60

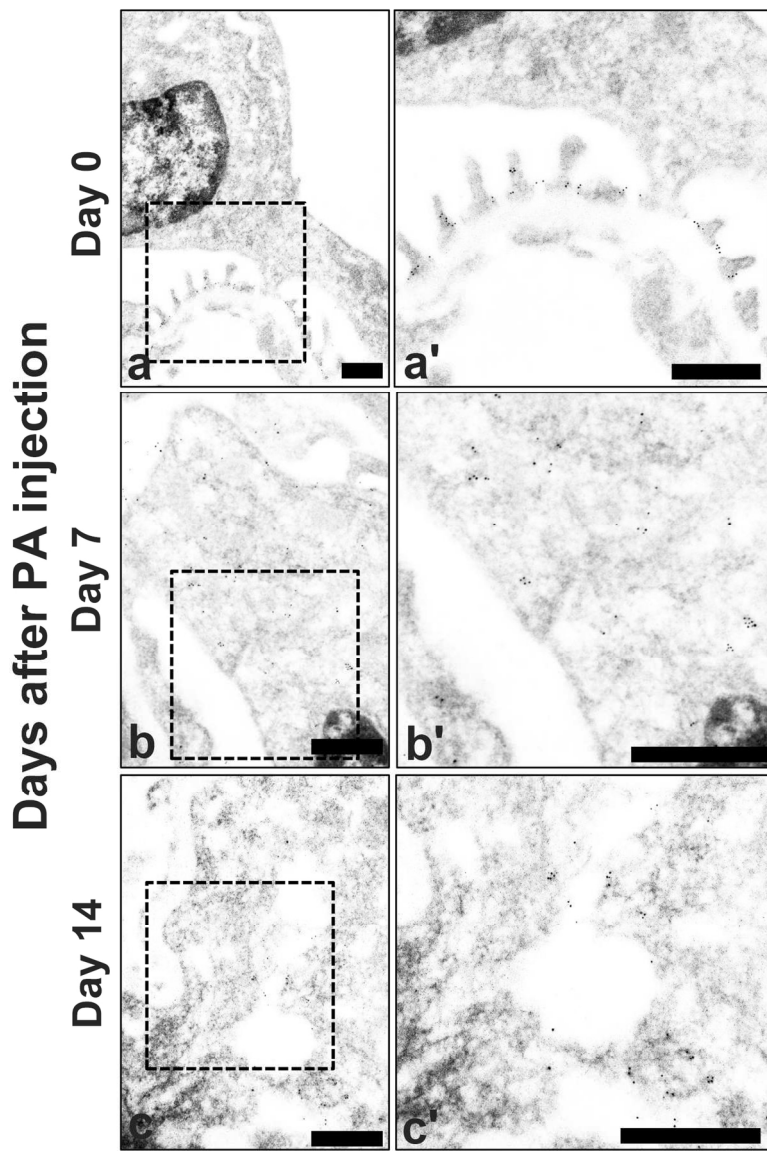


Fig. 3a-c: Immunoelectron microscopy of podocin in PAN rats. Podocin moved from the slit diaphragm area to the cytoplasmic area as form of vesicles at day 14 in the podocytes. Scale bar: 50nm (a-c, a'-c')

The left-side figure shows low magnification pictures ($\times 8000-20000$) and the right-side shows high magnification pictures ($\times 10000-50000$).

126x189mm (300 x 300 DPI)

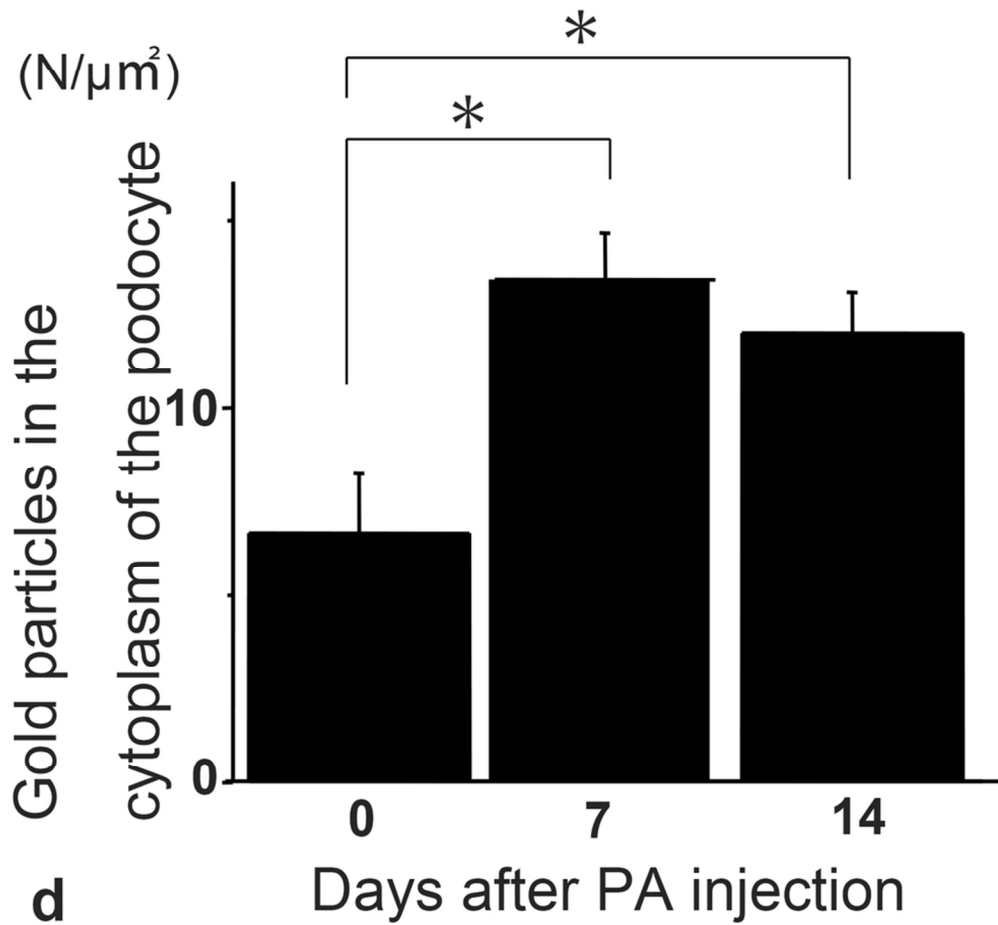


Fig. 3d: Podocin significantly moved to the cytoplasm of podocytes on days 7 and 14 in PAN rats. The number of gold particles (podocin) was calculated in the cytoplasmic area of podocytes. On days 7 and 14 podocin was significantly increased in the cytoplasmic area in podocytes ($n \geq 15$) ($p < 0.05$) (Mean \pm SE).

83x83mm (300 x 300 DPI)

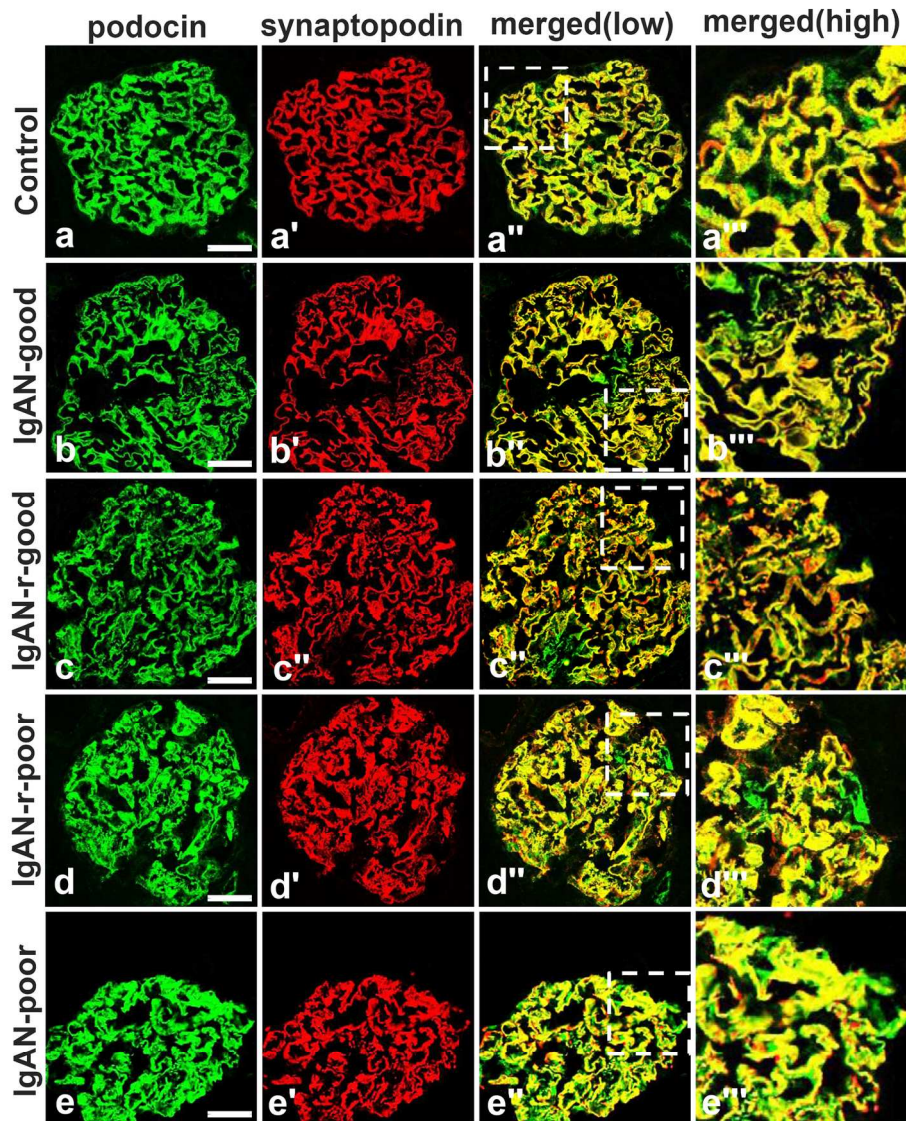


Fig. 4a-e: Double fluorescence of podocin (green), synpo (red), and merged (yellow) in IgA Nephropathy. In IgAN-good, -r-good, and -r-poor specimens, the staining area of podocin and synpo were almost the same, but the IgAN-poor podocin area (not merged with synpo, green) was larger than that of the other groups, and the staining pattern had changed from a linear type to cell body type. Scale bar: 50 μ m (a-e)

163x207mm (300 x 300 DPI)

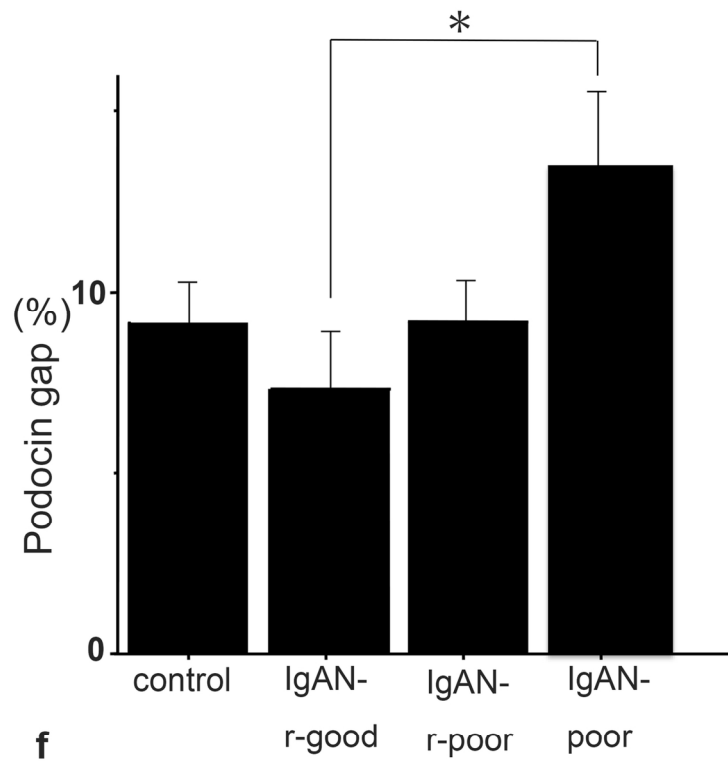


Fig. 4f: The changes in the discrepancy staining area with podocin and synpo in each prognosis categories of IgAN.

We measured the podocin gap (refer to Fig. 2f). In IgAN-r-good specimens, the gap was decreased as compared with that of the control, but interestingly in the IgAN-poor group the gap was significantly increased ($p < 0.05$) compared with that of IgAN-r-good control specimens, i.e. minor glomerular abnormality ($n \geq 4$) (Mean \pm SE).

149x174mm (300 x 300 DPI)

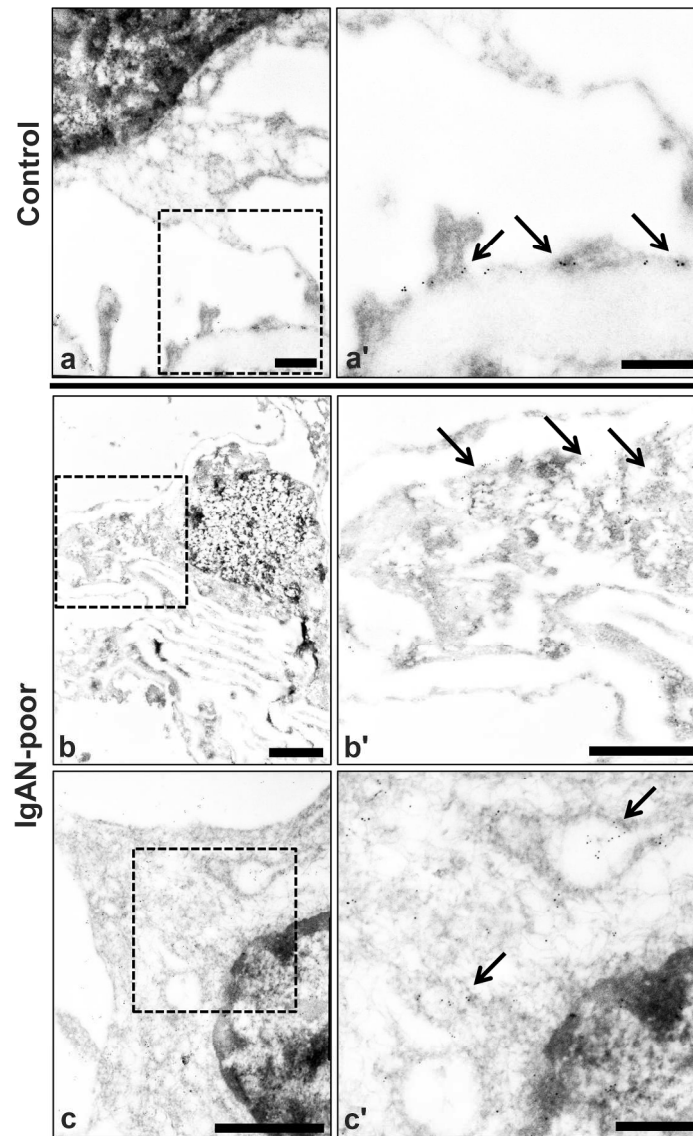


Fig. 5a-c: Immunoelectron microscopy of podocin in the control and IgAN-poor group. Podocin was translocated from the slit diaphragm area to the cytoplasmic area in the IgAN-poor group.

Scale bar: 500nm (a, a', c'), 2µm (b, b', c)

Normal glomerulus: minor glomerular abnormalities

The left-side figure shows low magnification pictures (×8000) and the right-side shows high magnification pictures (×30000).

199x310mm (300 x 300 DPI)

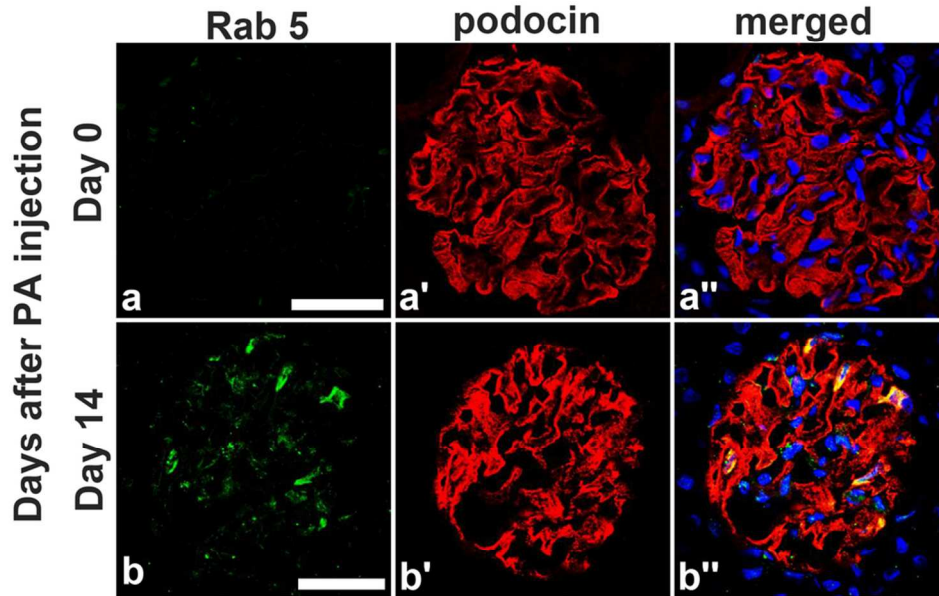


Fig.6a, b: Podocin and Rab5 merged in samples from day 14 PAN rats. We performed double staining of podocin and Rab, which is a specific early endosome marker, in day 14 PAN rats specimens, and detected several locations were podocin clearly merged with Rab5 (arrow). This suggests podocin translocation to the cytoplasm by endocytosis. Scale bar: 50 μ m (a, b)

91x64mm (300 x 300 DPI)

1
2
3
4
5
6
7
8
9
10
11
12
13
14
15
16
17
18
19
20
21
22
23
24
25
26
27
28
29
30
31
32
33
34
35
36
37
38
39
40
41
42
43
44
45
46
47
48
49
50
51
52
53
54
55
56
57
58
59
60

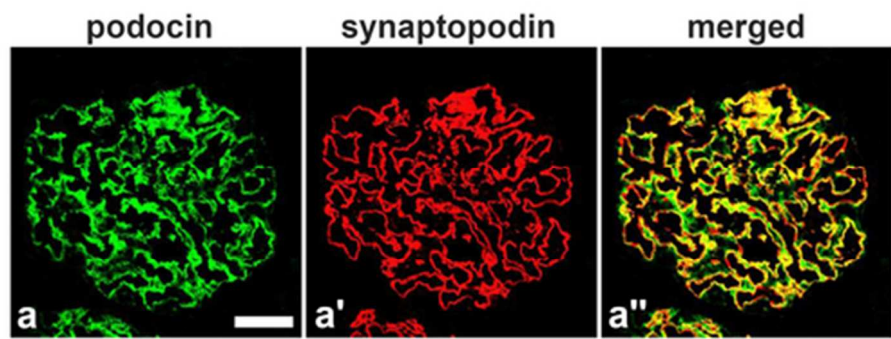


Fig.7: In human MCD podocin and synpo merged clearly and there was no significant podocin gap. Evaluation of the podocin gap in human MCD specimens showed that podocin and synpo stained the same foot process area. We did not find any evidence of podocin translocation. Scale bar: 50µm (a)

46x17mm (300 x 300 DPI)

Peer Review